Manuscript Number:

Title: Hybrid density functional calculations of hyperfine coupling tensor for hole-type defects in MgAl2O4

Article Type: VSI: REI-20

Section/Category: VSI: REI-20

Keywords: MgAl2O4 spinel; hole-type defects; hybrid DFT calculation; EPR

Corresponding Author: Dr. Denis Gryaznov,

Corresponding Author's Institution: Insitute of Solid State Physics, University of Latvia

First Author: Alexander Platonenko

Order of Authors: Alexander Platonenko; Denis Gryaznov, Dr; Eugene A Kotomin, Dr; Aleksandr Lushchik, Dr; Viktor Seeman, Dr; Anatoli I Popov, Dr

Abstract: We have performed the density functional calculations (DFT) to obtain the hole-type defects (V-centres) in magnesium aluminate spinel (MgAl2O4) following the results of recent paramagnetic resonance measurements (EPR) in Nucl. Inst. Methods Phys. Res. B 435 (2018) 31-37. The hybrid B3LYP functional calculations using large supercells of 448 atoms have demonstrated excellent results for not only bulk properties but also for the V-centres formation in MgAl2O4. Three types of V-centres have been considered and confirmed, namely V1, V2 and V22. The DFT calculations have revealed the atomic relaxation pattern and spin density around the hole-type defects that is suggested as an important complement to the experiments. Moreover, the calculated hyperfine coupling constants (HCCs) have been analyzed and compared with those from the measured EPR spectra. A good correspondence between the calculated and measured HCC values is discussed.

Hybrid density functional calculations of hyperfine coupling tensor for hole-type defects in $MgAl_2O_4$

Alexander Platonenko[a], Denis Gryaznov[a*], Eugene A. Kotomin[a], Aleksandr Lushchik[b], Viktor Seeman[b], Anatoli I. Popov[a]

[a] Institute of Solid State Physics, University of Latvia, 8 Kengaraga Str., Riga, LV-1063, Latvia
[b] Institute of Physics, University of Tartu, 1 W. Ostwald Str., Tartu, 50411, Estonia

ARTICLE INFO

ABSTRACT

We have performed the density functional calculations (DFT) on the hole-type defects (V-centres) in magnesium aluminate spinel ($MgAl_2O_4$) following the results of recent paramagnetic resonance measurements (EPR) in Nucl. Inst. Methods Phys. Res. B 435 (2018) 31-37. The hybrid B3LYP functional calculations using large supercells of 448 atoms have demonstrated excellent results not only for bulk properties but also properties of the V-centres in $MgAl_2O_4$. Three types of V-centres have been considered and confirmed, namely V_1, V_2 and V_{22}. The DFT calculations have revealed the atomic relaxation pattern and spin density distribution around the hole-type defects that is suggested as an important complement to the experiments. Moreover, the calculated hyperfine coupling constants (HCCs) have been analyzed and compared with those from the measured EPR spectra. A good agreement between the calculated and measured HCC values is observed and discussed.

1. Introduction

Magnesium aluminate spinel $MgAl_2O_4$ exhibits a very high tolerance to irradiation with fast neutrons due to the efficient recombination of primary radiation-induced Frenkel defects vacancies and interstitials, which makes it a promising material for optical/diagnostics windows in the environment of future fusion reactors. It is generally accepted that the accumulation of radiation-induced structural defects determines the radiation damage and strongly affects the functionality of various optical materials/components. In this connection, the investigation/understanding of the atomic and electronic structure of defects as well as their thermal annealing plays a crucial role.

Recently, it was discussed what happens with the defects formation in neutron-irradiated single crystals of $MgAl_2O_4$ [1]. The EPR measurements at room temperature helped to identify the intrinsic structural defects induced by the fast fission neutrons. The obtained values of *g*-tensor parameters allowed to conclude that the paramagnetic nature of the hole-type centers (called, for simplicity, V-centers in [1]) is supposed to be an O⁻ ion (i.e. a single hole trapped at a regular oxygen ion located near some negatively charged structural defect. Based on the experimentally measured angular dependencies for different V-centers and their comparison with the calculated ones in the "Easy Spin" program [2], the orientation of paramagnetic centers was determined and the following microstructures of hole containing centers were proposed [1, 3].

This study showed three different hole-type defects labeled as V_1, V_2, and V_{22}. In the case of V_1-centre a negatively charged defect is situated at the Al^{3+}-site which is the Al vacancy in the formal charge state -2, i.e. V_1-centre is a comlex V_{Al}^{-2} + O⁻. Similarly, the Mg vacancy in the formal charge state -1 is

associated with the V_2-centre = V_{Mg}^{-1} + O⁻. Also, the anti-site defect, when Mg^{2+} occupies the Al^{3+} position, showed up in the EPR spectra leading to a complex $V_{22} = M_g\big|_{Al}^{0}$ + O⁻. It can easily be understood that all the three V-centres are compensated by the formation of holes on oxygens to maintain the eletroneutrality condition.

The DFT calculations of EPR parameters for crystals is still rare in the literature [4, 5]. Previous calculations concerned mainly complex molecules in the cluster model, see, for example, [6, 7]. In the present study we rely on the implementation as suggested in the CRYSTAL17 computer code [8]. Notice that the calculation of *g*-tensor is not possible in CRYSTAL at the present stage but the HCCs can be calculated as demonstrated in careful study of defects in diamond [5]. Moreover, the DFT calculations could be used to deeper analyze the properties of such defects at atomistic level that is an important complement to experimental data. In previous study of Paudel et al. [9] the anti-site defects and of Jiang et al. [10] the oxygen vacancies in $MgAl_2O_4$ were calculated within the so-called DFT+U and G_0W_0 approach, respectively. Borges et al. [11] studied combinations of oxygen vacancy and anti-sites in different charge states by means of DFT and meta-GGA Becke-Johnson exchange potential. So, all these advanced DFT studies were focused on optical properties of defective $MgAl_2O_4$. Recently, the atomic and electronic structure of oxygen interstitial defects in $MgAl_2O_4$ was calculated by us using the hybrid DFT calculations [12, 13]. In the present study we decided to extend our hybrid DFT calculations to the V-centres and calculate, for the first time, the HCCs for a comparison with the those obtained from the measured EPR spectra.

2. Computational details

The formalism of linear combination of atomic orbitals (LCAO) combined with the hybrid B3LYP exchange-correlation functional was used in the present study of defects in $MgAl_2O_4$. The all-electron basis set of atomic Gaussian type functions in the form 8s-411sp, 8s-511sp and 8s-511sp-1d for O, Mg and Al respectively, were taken from the CRYSTAL web site (please see [14] and references therein). The primitive unit cell of $MgAl_2O_4$ consists of 14 atoms whereas its conventional unit cell consists of 56 atoms. We rely on the so-called supercell approach [15] and apply the transformation matrix (2 0 0, 0 2 0, 0 0 2) for the lattice translational vectors of the conventional unit cell. It leads to the supercell comprising 448 atoms. We choose a massively parallel version (MPP) of the CRYSTAL code based on a distributed-data approach [14]. Accordingly, the low symmetrical calculations due to the presence of defects in the supercell were performed with the one k-point mesh only in the Brillouin zone. The tolerances for the Coulomb and exchange integrals 6, 6, 6, 6, 12 and the SCF convergence threshold on the total energy 10^{-7} a.u. were used throughout all the spin-polarized calculations in the supercell. The primitive unit cell was calculated with the same tolerances but the k-point mesh 8x8x8.

The formation energy of a defect with a charge q was calculated in accordance with the following expression [16, 17]

$$\Delta E_F^q = E^q - E^{bulk} + E_{corr}^q - \sum_i n_i \mu_i + q(\varepsilon_F + \varepsilon_{VBM} + \Delta V),\quad (1)$$

where E^q and E^{bulk} represent the total electronic energies of supercells with a defect with a charge q and without a defect respectively, E_{corr}^q the finite-size supercell correction due to a first-order Makov-Payne scheme. The calculation of formation energy requires consideration of the chemical potential μ_i of n_i species and the chemical potential of electrons (term in the parentheses) removed or added. Therefore, ε_F and ε_{VBM} stem for the Fermi energy and valence band maximum of perfect crystal, respectively. In our study, we use the chemical potential of O μ_O equal half the O_2 molecule total energy, μ_{Al} found from the total energy of α-Al_2O_3 phase, and μ_{Al} from the total energy of MgO. Notice that the bond length and binding energy of O_2 are accurately calculated with the LCAO approach and hybrid functionals [18]. ΔV is a correction for the average electrostatic potential alignment between the supercells with and without a defect. As was shown in [17] ΔV decreases rapidly with the supercell sizes in wide bandgap materials. In our present calculations, ΔV is very small (of the order of 0.01 V) due to a large supercell size of 448 atoms. Charged supercells were calculated with a homogenous neutralizing charge background.

The hyperfine coupling tensor can be calculated through the spin Hamiltonian as discussed in detail in [5]. Below we present the isotropic contribution A^{iso} (the Fermi contact term) to the tensor and the anisotrpic dipole-dipole interaction of the electron with the nuclear spin B (or its components B_x, B_y, B_z). The hyperfine coupling tensor (A_x, A_y, A_z) is given by their combination through the identity matrix and is calculated for a comparison with experimental data in [1]. Therefore, the combination can be given by the following expression [19]

$$\begin{pmatrix} A_x & 0 & 0 \\ 0 & A_y & 0 \\ 0 & 0 & A_z \end{pmatrix} = A^{iso} + \begin{pmatrix} B_x & 0 & 0 \\ 0 & B_y & 0 \\ 0 & 0 & B_z \end{pmatrix}. \quad (2)$$

3. Results and discussion

3.1. Basic bulk properties of $MgAl_2O_4$

Magnesium aluminate $MgAl_2O_4$ crystallizes in the spinel structure (space group 227, $Fd\bar{3}m$) which is a face-centered cubic lattice. Its primitive unit cell contains the Mg atoms occupying Wyckoff position 2a (1/8, 1/8, 1/8), Al atoms occupying Wyckoff position 4d (1/2, 1/2, 1/2), and O atoms occupying Wyckoff position 8e (x, x, x) with one free parameter. The calculated lattice constant a of 8.15 Å using the B3LYP functional for the primitice unit cell is little larger than the experimental value of 8.06 Å [19] whereas the free parameter x agrees very well with the experimental value. It should be mentioned that the conventional DFT functional suffers from the error of underestimated bandgap value (Δ). Recently, Jiang et al. [10] included man-body effects within the G_0W_0 approximation whereas Borges et al. [11] applied meta-GGA Becke-Johnson exchange functional to reproduce the Δ-value. Alternatively, the hybrid density functionals (like those B3LYP and range-separated HSE06) accounting for the exact exchange could be used to solve the problem of bandgap. Even though a calculated with the HSE06 functional is closer to the experimental value in comparison with the B3LYP functional, Δ does the opposite effect [12]. Notice that the Δ-value as obtained with the HSE06 functional is almost by 1 eV larger than the experimental value of 7.80 eV and the G_0W_0-value of 7.88 eV [10].

Table1. Basic bulk properties of $MgAl_2O_4$ as calculated with the B3LYP functional in the present study and compared with the experiments in the literature. a the lattice constant, x the free parameter, Δ the electronic band gap and Q the effective atomic charge.

Property	Present study	Experiment
a / Å	8.15	8.06[a]
x	0.26	0.26[a]
Δ/ eV	7.68	7.80[b], 8.20[c,d]
Bond length / Å	Al-O: 1.92-1.94 Mg-O: 1.96	
Q / e	Mg: +1.83 Al: +2.29 O: -1.61	-

[a] Ref. 20 [b] Ref. 21 [c] Ref. 22 [d] Ref. 23

Unfortunately, the effective atomic charges (Q) are rarely discussed in the literature. Nevertheless, the Q-values give us important information on bonding in a compound. So, Q's calculated in the present study with the Mulliken analysis and B3LYP functional being different from the formal ones (2+ for Mg and 3+ for Al) suggest quite covalent picture for the Al-O bond and more ionic picture for the Mg-O bond. These atomic charges for both the bonds, however, are more ionic in comparison with those calculated with the HSE06 functional [13].

3.2. Calculations of V-centres in $MgAl_2O_4$

In table 2 we collected the basic properties of defective $MgAl_2O_4$ containing one of the three V-centres: $V_1 (= V_{Al}^{-2} + O^-)$, $V_2 (= V_{Mg}^{-1} + O^-)$, and $V_{22} (= Mg|_{Al}^0 + O^-)$. Therefore, the basic properties were calculated in the supercell comprising 447 atoms. In particular, we emphasize the atomic charge Q and magnetic moment M of oxygen with the localized (trapped) hole (O^-) due to

1 missing electron in the system. The magnetic moment M of O⁻ is larger for the cation vacancies case than the anti-site defect, but Q of O⁻ is larger for the anti-site defect than for the cation vacancies. If we compare the two cation vacancies, then the larger Q of O⁻ for V_1 than for V_2 could be understood from the formal charge state: the Al vacancy charge state -2 for V_1 means more electrons left in the system in comparison with the Mg vacancy charge state -1. Consequently, the more oxidized cation has slightly smaller value of M. Interestingly, calculations of the defective supercells of different sizes did not reveal any significant changes in their properties.

Table 2. The poperties of calculated V-centres in $MgAl_2O_4$. Q and M the affective atomic charge and magnetic moment of oxygen ion with the localized (trapped) hole (O⁻).

Defect	Q / e	M / μ_B
V_1	-0.92	0.78
V_2	-0.78	0.80
V_{22}	-1.05	0.72

Fig. 1. (Color online) 2D spin density maps (left) for V_1- (a), V_2- (b), V_{22}- (c) centres and corresponding atomic relaxation patterns (right) around O⁻ defects. On right: red balls O ions, gray balls Al ions, green balls Mg ions and anti-site, dark red ball O⁻, light gray ball Al vacancy (a), dark green ball Mg vacancy (b). There is an effective atomic charge in e for each ion on right whereas the numbers marked in bold show inter-atomic distances in Å.

One could understand from the values of M that there is some part of the hole donated to other ions in the system. The formal magnetic moment M of O⁻ would be 1 μ_B. In order to better analyze this effect we plotted the spin density distribution around O⁻ for each V-center (fig. 1). As expected the maximum spin density is observed at the O⁻ ion in all the three cases. It is reflected in the highest intensity of the isolines around O⁻. But, there is also a non-zero spin density localized at oxygens which are neighbours of O⁻. In addition, we found small magnetic moments for such oxygens. The analysis of oxygen neighbors for each V-center, their magnetic moments and the atomic charges suggests the following picture. The case of V_1: the larger $M(Q)$ of 0.06 μ_B (-1.42 e) for two oxygens which are neighbours for both the Al vacancy and O⁻ (4th and 5th oxygen neighbour for O⁻, not the nearest oxygen neighbours) and the smaller $M(Q)$'s of 0.01(-1.59 e), 0.02 μ_B (-1.46 e) and 0.03 μ_B (-1.54 e). The case of V_2: the larger $M(Q)$ of 0.05 μ_B (-1.54 e) for three oxygens which are nearest oxygen neighbours for O⁻, and the smaller $M(Q)$'s of 0.01 μ_B (-1.28 e) which are nearest oxygen neighbors for the Mg vacancy. The case of V_{22}: the larger $M(Q)$ of 0.06 μ_B (-1.51 e) for two oxygens which are second nearest oxygen neighbours for O⁻, the smaller $M(Q)$'s of 0.022 (-1.598 e), 0.039 μ_B (-1.574 e), 0.000 (-1.627 e) which are nearest oxygen neighbors for the anti-site defect, $M(Q)$'s of 0.015 (-1.548 e), 0.039 (-1.573 e) which are 3rd and 4th oxygen neighbors for O⁻. The obtained atomic charges are much different from the values in the perfect bulk material and should, therefore, be carefully analyzed. Different values of M's for oxygens are reflected in the intensity of isolines in fig. 1 as well.

The inter-atomic distances between the cation vacancy and neighbouring oxygen ions (fig. 2) are close for both the Al and Mg vacancy, i.e. the relaxation pattern is quite symmetric. The difference in relaxation patterns for the two cation vacancies is reflected in larger inter-atomic distances in case of the Al vacancy including the distance between that vacancy and O⁻ (2.09 Å vs 2.19 Å in fig. 1 on right). As expected, all these inter-atomic distances are larger than in perfect bulk material (table 1) as the oxygens move apart from each other upon the formation of cation vacancy. The anti-site defect experiences more complex changes reflected in a quite asymmetric relaxation pattern. The distance between the anti-site defect and O⁻ is even larger than that in the case of cation vacancies.

As can be seen in the spin density maps, oxygens on larger distances do not contain the holes. So, this part of the hole seen on the oxygen neighbours of O⁻ is not delocalized over a whole supercell but rather localize on them. In table 3 we present calculated HCCs and experimental values from [1] for a comparison. Almost equal components of the hyperfine coupling tensor were discussed in [1] and are confirmed here for all the three cases of V-centres despite the low-symmetric supercells. It indicated independence of the direction of the applied magnetic field. Notice that the V_1 and V_{22}-centres were calculated in the supercells without imposing the symmetry constraints. The isotropic contribution A^{iso} should be larger than the anisotropic dipole-dipole interaction B [19]. However, we emphasize one order of magnitude difference between A^{iso} and B (A^{iso} = -0.60 mT vs B_x = - 0.03 mT, B_y = -0.05 mT, B_z = -0.08 mT, for example). We suggest a good agreement between the measured and calculated HCCs. It should be noticed that determination of HCCs from the measured EPR spectra is a rather complicated procedure. The complicity is caused by the overlap of the spectra. The V-centres are differently oriented with respect to the applied magnetic field, and there is a mixture of the overlapping spectra. Only certain amount of lines belonging to the concrete orientation of a certain V-center with respect to applied magnetic field can be

used for the determination of EPR parameters. Thus, the DFT calculations help to not only calculate the properties of defects but also confirm their existence.

Table 3. The calculated HCCs of Al ion for three V-centres and their comparison with experimental values (in parentheses) from [1]. A_x, A_y, A_z were calculated using Eq. 2. We give the HCCc for Al ion being the nearest neighbour of O^-.

Defect	A^{iso} / mT	A_x / mT	A_y / mT	A_z / mT
V_1	-0.60	-0.63 (0.86)	-0.65 (0.86)	-0.68 (0.93)
V_2	-0.71	-0.72	-0.71	-0.60
V_{22}	-0.58	-0.62 (0.45)	-0.60 (0.45)	-0.63 (0.46)

3.3. Calculations of formation energy of V-centres in $MgAl_2O_4$

We calculated the formation energy ΔE^q_F (Eq. 1) of cation vacancies and anti-site in different charge states as shown in fig. 1. In fig. 1 the charge state -2 for the Al vacancy means formation of the V_1-centre, the charge state -1 for the Mg vacancy means formation of the V_2-centre, and the charge state 0 for the Mg anti-site means formation of the V_{22}-centre. As expected ΔE^q 's of cations are lowest in the highest charge states. And, it is energetically most unfavourable to consider the neutral cation vacancies when the largest number of localized holes is formed in the supercell. The overall picture suggests that ΔE^q 's of both the cations are close in corresponding charge states. Only appearance of the charge state -3 for the Al vacancy makes this vacancy more energetically favourable in comparison with the Mg vacancy with the charge state -2. However, our main interest lies in the O^- ion (i.e. a single hole trapped at a regular oxygen ion). Correspondingly, the Al vacancy with the charge state -2 is little easier to form than the Mg vacancy with q = -1 e. But, both the cation vacancies concede this formation energies competition the anti-site defect independently of their charge state. We should mention that ΔE^q of $V_{22} = M_g \big|^0_{Al} + O^-$ is by almost a factor of 2 smaller than ΔE^q of $V_2 = V^{-1}_{Mg} + O^-$ and by almost 1 eV smaller than ΔE^q of $V_1 = V^{-2}_{Al} + O^-$. As discussed in Ref. 4, it could be explained by the fact the two cations have close ionic radii in spinels, and it is easier to replace one by the other than to break the bond. Notice that there is energetic preference of the "+1" charge state for the anti-site defect at the ε_F-values smaller than 2 eV and, as a result, a very tiny region for the energetic preference of the "0" charge state of V_{22}. The "+1" charge state stable at smaller ε_F was earlier seen in other spinels as well [21].
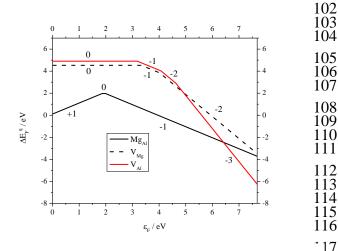

Fig. 2. Formation energy of V_{Al}, V_{Mg} and Mg_{Al} in different charge states a function of Fermi energy ε_F (Eq. 1) calculated with the B3LYP functional.

4. Conclusions

The hybrid DFT B3LYP calculations were performed in order to calculate and analyze properties of hole-type defects in $MgAl_2O_4$. The hybrid B3LYP functional reproduced not only the lattice parameters but also the bandgap of $MgAl_2O_4$. The main focus was placed on the calculation of V-centres with the single hole trapped on a regular oxygen ion (O^-) in accordance with the previous experimental observations. We confirmed that such defects could be present in $MgAl_2O_4$. Moreover, the calculated hypefine coupling constants (HCCs), the atomic and electronic structure of calculated defects are consistent with the measured ones [1]. In accordance with the calculated spin density maps we showed that the hole is only partly localized at O^- whereas, and there is its insignificant part donated to neighboring oxygen ions. The latter fact is important for understanding the values of calculated HCCs. The calculated HCCc confirm existence of calculated V-centres as their identification from the measured EPR is rather complicated.

References

1. A. Lushchik, S. Dolgov, E. Feldbach, A. I. Popov, E. Shablonin, V. Seeman, Creation and thermal annealing of structurel defects in neutron-irradiated $MgAl_2O_4$ single crystals. Nucl. Inst. Methods Phys. Res. B 435 (2018) 31-37.

2. www.easyspin.org

3. V. Seeman. E. Feldbach, T. Kärner, A. Maaroos, N. Mironova-Ulmane, A. I. Popov, E. Shablonin, E. Vasil'chenko, A. Lushchik, Fast-neutron-induced and as-grown structural defects in magnesium aluminate spinel crystals with different stoichiometry. Optical Materials 91 (2019) 42-49.

4. K. Szász, X. T. Trinh, N. T. Son, E. Janzén, A. Gali, J. Appl. Phys. 115 (2014) 073705.

5. A. M. Ferrari, S. Salustro, F. S. Gentile, W. C. Mackrodt, R. Dovesi, Substitutional nitrgen in diamond: A quantum mechanical investigation of the electronic and spectroscopic properties. Carbon 134 (2018) 354-365.

6. W. M. Ames, S. C. Larsen, DFT Calculations of EPR Parameters for Copper(II)-Exchanged Zeolites Using Cluster Model. J. Phys. Chem. A 114 (2010) 589-594.

7. H. H. Haeri, I. Bogeski, R. Gulaboski, V. Mirceski, M. Hoth, R. Kappl, An EPR and DFT study on the primary radial formed in hydorxilation reactions of 2,6-dimethoxy-1,4-benzoquinone. Molecular Physics 114 (2016) 1856-1866.

8. R. Dovesi, V.R. Saunders, C. Roetti, R. Orlando, C.M. Zicovich-Wilson, F. Pascale, B. Civalleri, K. Doll, N.M. Harrison, I.J. Bush, Ph. D'Arco, M. Llunell, M. Causà, Y. Noël, L. Maschio, A. Erba, M. Rerat, S. Cacassa, CRYSTAL17 User's Manual (University of Torino, 2017).

9. T. R. Paudel, A. Zakutayev, S. Lany, M. d'Avezac, A. Zunger, Doping rules and Doping Prototypes in A_2BO_4 Spinel Oxides. Adv. Funct. Mater. 21 (2011) 4493-4501.

10. S. Jiang, T. Lu, Y. Long, J. Chun, Ab initio many-body study of the electronic and optical properties of $MgAl_2O_4$ spinel. J. Appl. Phys. 111 (2012) 043516.

11. P. D. Borges, J. Cott, F. G. Pinto, J. Tronto, L. Scolfaro, Native defects as sources of optical transitions in $MgAl_2O_4$ spinel. Mater. Res. Express 3 (2016) 076202.

12. R. A. Evarestov, A. Platonenko, Yu. F. Zhukovskii, Site symmetry approach applied to the supercell model of $MgAl_2O_4$ spinel with oxygen interstitials: *Ab initio* calcualtions. Comp. Mater. Science 150 (2016) 517-523.

13. A. Platonenko, D. Gryaznov, Yu. F. Zhukovskii, E. A. Kotomin, First Principles Simulations on Migration paths of Oxygen Interstitials in $MgAl_2O_4$. Phys. Status Solidi B 256 (2019) 1800282.

14. www.crystal.unito.it

15. R. A. Evarestov, Quantum Chemistry of Solids. Springer: Heidelberg, 2013.

16. H.-P. Komsa, T. T. Rantala, A. Pasquarello, Finite-size supercell correction schemes for charged defect calculations. Phys. Rev. B 86 (2012) 045112.

17. T. R. Durrant, S. T. Murphy, M. B. Watkins, A. L. Shluger, Relation between image charge and potential alignment corrections for charged defects in periodic boundary conditions. J. Chem. Phys. 149 (2018) 024103.

18. D. Gryaznov, E. Blokhin, A. Sorokine, E. A. Kotomin, R. A. Evarestov, A. Bussman-Holder, J. Maier, A Comparative Ab Initio Thermodynamic Study of Oxygen Vacancies in ZnO and $SrTiO_3$: Emphasis on Phonon Contribution. J. Phys. Chem. C 117 (2013) 13776-13784.

19. C. C. Rowlands, D. M. Murphy, EPR Spectroscopy, Theory in Encyclopadia of Spectroscopy and Spectrometry, Third Ediition. Elsevier Ltd, 2017.

20. M. Ishii, J. Hiraishi, T. Yamanaka, Structure and lattice vibrations og Mg-Al spinel solid solution. Phys. Chem. Minerals 8 (1982) 64-68.

21. M. L. Bortz, R. H. French, D. J. Jones, R. V. Kasowski, F. S. Ohuchi, Temperature dependence of the electronic structure of oxides: MgO, $MgAl_2O_4$ and Al_2O_3. Phys. Scr. 41 (1990) 537-541.

22. G. Prieditis, E. Feldbach, I. Kudryavstseva, A. I. Popov, E. Shablonin, A. Lushchik, Luminescence characteristics of magnesium aluminate spinel crstals of different stoichiometry. IOP Cond. Ser.: Mater. Science Eng. 503 (2019) 012021.

23. E. Feldbach, I. Kudryavstseva, K. Mizohata, G. Prieditis, J. Räisänen, E. Shablonin, A. Lushchik, Optical Characteristics of virgin and proton-irradiated ceramics of magnesium aluminate spinel. Optical Mater. 96 (2019) 109308.

24. D. Muñoz Ramo, P. D. Bristowe, The effect and disorder on the electronic properties of $ZnIr_2O_4$. J. Chem. Phys. 141 (2014) 084704.

Declaration of interests

☒ The authors declare that they have no known competing financial interests or personal relationships that could have appeared to influence the work reported in this paper.

☐The authors declare the following financial interests/personal relationships which may be considered as potential competing interests: